*J. Fluid Mech.* (1998), *vol.* 361, *pp.* 333–349. Printed in the United Kingdom



# Laminar–turbulent transition in Poiseuille pipe flow subjected to periodic perturbation emanating from the wall

By S. ELIAHOU, A. TUMIN AND I. WYGNANSKI†

Department of Fluid Mechanics and Heat Transfer, Tel-Aviv University, Tel-Aviv 69978, Israel

(Received 26 November 1996 and in revised form 6 January 1998)

Transition in fully developed circular pipe flow was investigated experimentally by the introduction of periodic perturbations. The simultaneous excitation of the azimuthal periodic modes $m = +2$ and $m = -2$ was chosen for detailed analysis. The experiments were carried out at three amplitudes. At the smallest amplitude the disturbances decayed in the direction of streaming. At intermediate input amplitude the disturbances amplified initially but then decayed with increasing distance downstream. Their growth was accompanied by the appearance of higher harmonics. At still higher amplitudes transition occurred. A mean velocity distortion corresponding to an azimuthal index of $m = 4$ was observed at the intermediate and at the higher levels of forcing. When four stationary jets were introduced through the wall to emulate a similar mean velocity distortion, transition was observed at smaller amplitudes of forcing at modes $\pm 2$. Thus, weak longitudinal vortices provide an added instability needed to generate a secondary disturbance which, in turn, amplifies the steady vortical structures introduced by the jets. Such vortices may also be generated through the interaction of time-periodic helical modes.

## 1. Introduction

Laminar–turbulent transition of pipe flow is still an enigma in fluid mechanics. Reynolds (1883) observed that laminar pipe flow becomes turbulent when a dimensionless quantity later bearing his name $Re = \varrho D U_m/\mu$, based on mean velocity $U_m$ and pipe diameter $D$, was large enough. It was established that there is a critical Reynolds number of about 2000 below which transition from a laminar to turbulent state does not occur regardless of the initial disturbance amplitude. At low level of disturbances the transition Reynolds number could be much larger than the critical value of 2000. Further investigations have shown that a pipe flow might be laminar even at $Re$ about $10^5$ (Pfeninger 1961) and the character of the flow depends on the disturbance amplitude at the pipe inlet (Wygnanski & Champagne 1973). Wygnanski & Champagne investigated transitional pipe flow and found two different types of turbulent structures. There are slugs generated at supercritical $Re$ by the instability of the flow at the inlet, and puffs generated by large disturbances around the critical $Re$. The structure of puffs was investigated by Wygnanski, Sokolov & Friedman (1975) and later by Rubin, Wygnanski & Haritonidis (1980) with the help of strong momentary excitation introduced at the inlet, and later in the fully developed region.

† Also Department of Aerospace and Mechanical Engineering, The University of Arizona, Tucson, Arizona 85721, USA.

Actually, there are two distinctly different transition experiments to be considered: transition due to disturbances in the inlet region, and transition in fully developed Poiseuille flow. The inlet region in laminar flow may extend over a few hundred diameters because its length depends on Reynolds number. Theoretical investigations of the inlet flow by Goldstein (1938) and Christiansen & Lemmon (1965) were based on steady-state equations, but Wygnanski & Champagne (1973) showed that initial disturbance levels at the inlet are important for the evolution of a parabolic velocity profile. Because of the evident importance of the inlet region, and because all theoretical investigations (see Drazin & Reid 1981) pointed out the stability of the Poiseuille flow, Morkovin & Reshotko (1990) suggested that the most likely bypasses are to be found in the linearly, weakly unstable, slowly accelerating boundary layers before the parabolic velocity profile was attained. Nevertheless, transition due to a strong disturbance in fully developed flow is possible and the mechanism of turbulence onset in this flow is yet to be determined.

Stability experiments with disturbances introduced in the fully developed region of the pipe flow were carried out by Leite (1959), Reshotko (1958) and Kaskel (1961). Leite used a mechanical disturbance generator located near the inner wall. It introduced small nearly axisymmetric disturbances into the flow. The measurements of the disturbance amplitude in the radial and longitudinal directions were carried out by a single hot-wire probe. The experiments showed that small-amplitude disturbances decayed in the flow. To generate axially symmetric disturbances of larger amplitude, a ring airfoil was mounted within a cylindrical sleeve, and a transition was observed subsequent to an increase in Reynolds number. Kaskel also used a mechanical disturbance generator composed of six equally spaced reeds that generated an almost symmetrical disturbance. A transient growth of some excited disturbances that decayed further downstream was observed in the experiments. Fox, Lessen & Bhat (1968) employed an oscillating small vane (whose plane was parallel to the tube axis and whose motion was perpendicular) in the entrance region. The disturbance generator excited mainly two azimuthal modes of indices $m = \pm 1$. They concluded that the disturbances could be unstable and established a 'neutral curve' in the 'frequency–Reynolds number' plane. Rubin *et al.* (1980) introduced a pulsed disturbance into a fully developed Poiseuille flow and concluded that the resulting transitional flow was similar to the flow disturbed at the inlet. Darbyshire & Mullin (1995) extended the previous experiments with disturbances introduced into fully developed pipe flow. They established that a critical amplitude of the disturbance was required to cause transition, and that it depended on Reynolds number. The qualitative result requiring a threshold amplitude to cause transition agrees with the numerical simulations describing the onset of turbulence in a pipe (Boberg & Brosa 1988). A common deficiency of the above-mentioned experiments is the absence of information about the character of the disturbances, their spectral content, their distribution across the pipe and their azimuthal distribution downstream from the generator. Also, there is no information about mean velocity profiles in the transition zone in the presence of the disturbances, regardless of their size and intensity.

New attempts to explain transient growth have been made recently. Such growth may even be predicted by linear models in fully developed pipe flow. Gustavsson (1989) considered the possibility of direct resonance between pressure eigenmodes and streamwise velocity components. Since certain eigenvalues obtained from the equation describing the pressure disturbance may coincide with eigenvalues of the uniform equation for the streamwise component of the velocity disturbance, an algebraic growth may occur at the initial stages of the development of such a

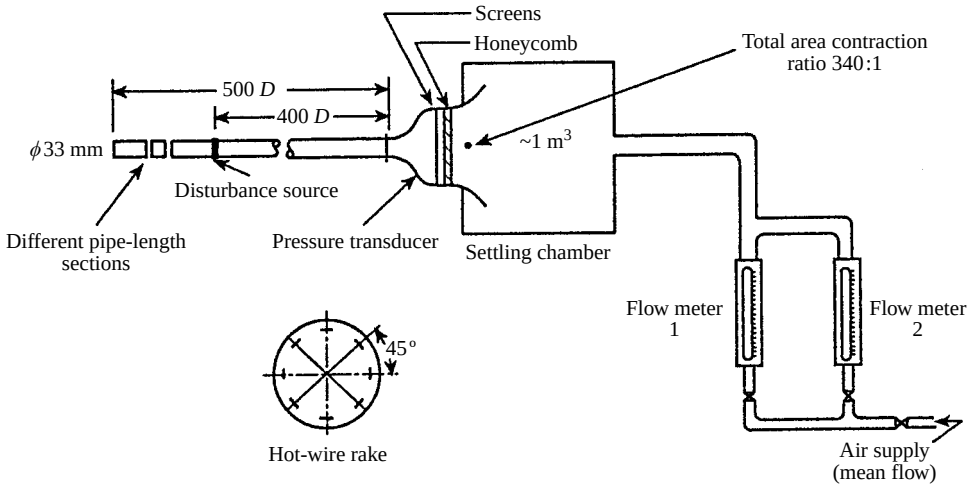


FIGURE 1. A sketch of the pipe facility.

disturbance. A more general mechanism of the transient growth was investigated by Bergström (1992). The results for an optimal transient growth in Poiseuille pipe flow were published by Bergström (1993*a*) and by Schmid & Henningson (1994). In order to find transient growth in an experiment, Bergström (1993*b*) investigated the evolution of a localized disturbance in a pipe flow. Although a transient growth was observed by him and by Kaskel (1961), it is not clear that the results are applicable to the linear regime of the disturbance. Neither the spectra nor the distortions of the mean velocity profile were measured in the presence of the transient disturbances. Although Mayer & Reshotko (1997) succeeded in fitting the experimental data of Kaskel with a proper combination of linear eigenfunctions, the applicability of the linear model to the experiments of Kaskel remains unclear.

Recently, Waleffe (1995*a*, *b*, 1996) suggested that the transition in linearly stable shear flows may be associated with a self-sustaining process (SSP). He illustrated the idea for a plane Couette flow where weak streamwise rolls excited by the input disturbance redistribute the streamwise momentum causing non-uniformity along the span. The flow is unstable with respect to the three-dimensional wave-like disturbances that, in turn, sustain the streamwise rolls. In the case of a pipe flow the SSP includes the generation of azimuthal fluctuations in the streamwise velocity component, which are analogous to the spanwise variations in plane Couette flow.

Longitudinal rolls play an important role in pipe transition according to Nikitin (1994, 1995), who drew his conclusions from a numerical simulation of the flow. Zikanov (1996), who studied numerically the stability of a pipe flow in the presence of longitudinal rolls, established that the flow may be unstable with respect to infinitesimal three-dimensional disturbances. These results are consistent with the SSP scenario.

The object of the present paper is to consider the evolution of periodic perturbations of variable intensity in a fully developed Poiseuille pipe flow. The experiments were carried out at a slightly supercritical Reynolds number of about 2200 and the disturbances were introduced through slots milled in the pipe wall located 400 diameters downstream of the inlet. The azimuthal distribution of the flow perturbations and their effect on the mean velocity were carefully determined

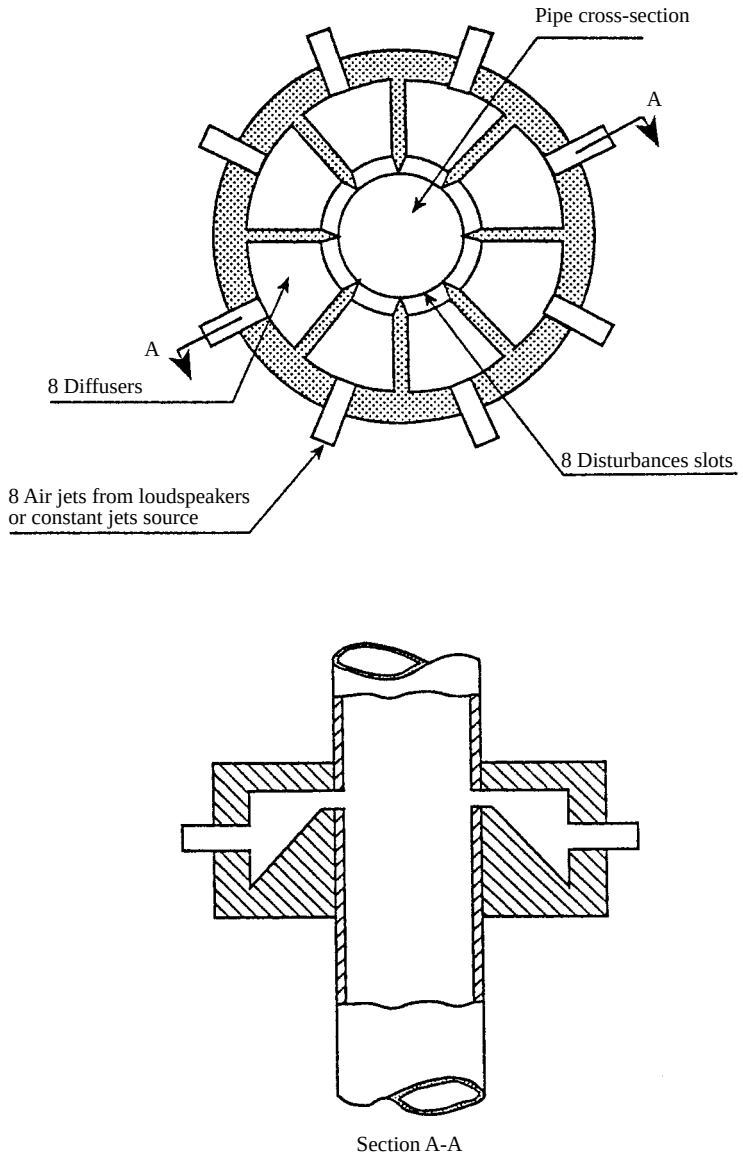


FIGURE 2. A schematic sketch of the disturbance generator surrounding the pipe.

## 2. Apparatus and instrumentation

The experiments were carried out in an aluminium pipe 33 mm in diameter and 17 m long. The facility was initially described in the paper by Wygnanski & Champagne (1973) and is shown schematically in figure 1. The flow was supplied by a high-pressure source (6 atm compressor) through a flow-meter and a differential pressure controller and passed through a settling chamber to the pipe. The mass flux through the system was regulated by a diaphragm. A disturbance generator was placed at $X/D = 400$, where $X$ is the distance from the pipe inlet. The disturbances were generated by eight acoustic drivers independently controlled by adjustable amplifiers to provide identical frequencies and amplitudes at prescribed phase shifts. The disturbances generated by

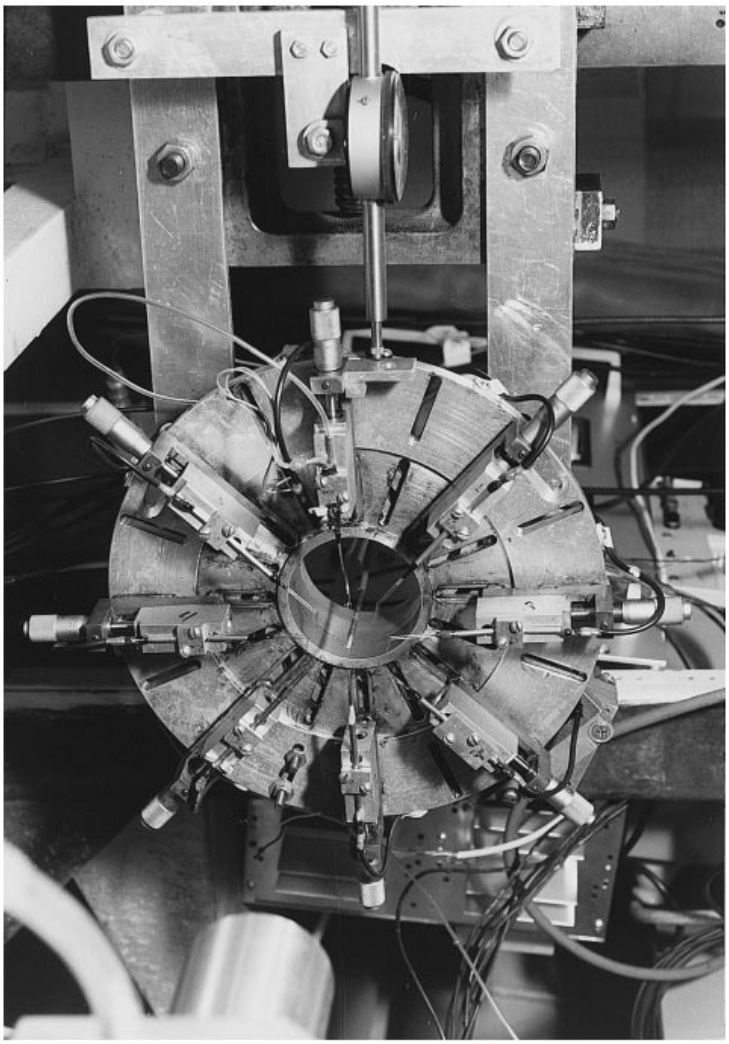

FIGURE 3. Hot-wire rake and traverse.

each of the drivers displaced the air in a corresponding settling chamber which, in turn, was accelerated in a contraction leading to a slot in the pipe surface. Thus, periodic suction and blowing was generated through the slots which covered 45° of the azimuthal angle and whose width was 2 mm (see figure 2). The adjustable phase shift allowed the generation of different helical modes in the pipe. To observe the development of the disturbances at various distances from the generator, a few interchangeable pieces of pipe were affixed to the main pipe section at the source location.

Measurements were done using a multichannel hot-wire anemometer system. To reduce the size of the probes, jeweller broaches were used as prongs. Each of them was soft soldered to a fine copper wire and enclosed in a thin stainless steel tube, instead of the traditionally used ceramic tube. The hot wires were made of tungsten and were 5 μm in diameter with an aspect ratio of 300.

The hot-wire rake (see figure 3) consisted of eight normal hot wires displaced

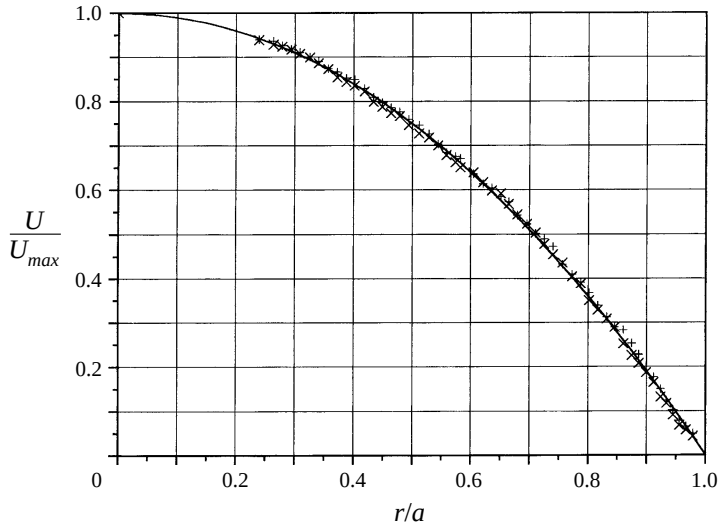


FIGURE 4. Laminar mean velocity profile. $Re = 2280$; distance from the disturbance generator $x/D = 1.82$. Symbols, experiment; line, parabolic profile.

at equal circumferential angles in a ring-like arrangement. The eight probes were mounted on separate micrometer screws and could be independently adjusted in both the radial and axial directions. A ninth hot wire was placed on the pipe axis. The minimum radial distance at which all probes could operate without interference was $r/a \approx 0.25$ ($a$ is the pipe radius). Thus, there is no simultaneous data available at $r/a < 0.25$ with the exception of the hot wire located on the centreline. Radial alignment of the probes was accomplished by blocking the pipe exit with a plug containing eight (precisely milled) small holes 0.2 mm in diameter and by adjusting the position of each of the eight hot wires to sense the small jet emanating from these holes. The traversing mechanism was able to move all sensors simultaneously an equal distance in the radial direction. The radial position of the probes was controlled by a computer connected to a stepper motor. The ring assembly of the probes could be translated in the axial direction along two guide posts that were aligned with the pipe axis. All velocity measurements were done at the exit plane of the pipe.

The hot wires operated at constant-temperature mode with an overheat of 1.5 and their output signal was low-pass filtered at 10 kHz. The calibration of the eight probes was done at $r/a = 0.25$, while the ninth probe was done at the centreline. The probes were calibrated against the local dynamic pressure monitored by a MKS Baratron transducer. The variation of the anemometer voltage output with velocity was approximated by a fourth-order polynomial. The calibration was carried out at seven velocities ranging from 10 cm $s^{-1}$ to 3 m $s^{-1}$. The data from the nine hot-wire probes together with a reference signal were digitized and stored on a PC. The disturbance signal was used for phase reference. Fourier analysis in time and in azimuthal angle was performed to provide information about the various azimuthal modes of the various frequencies.

The signals were generated by a computer interface board made by the National Instruments Corporation. The ten independent 12-bit voltage output channels of this board were used as a voltage source for a prescribed signal generation. The output

signal was then amplified by a ten channel power amplifier, built at the Tel-Aviv University for activating the loudspeakers. The resulting pressure perturbation in each settling chamber was independently monitored in order to calibrate the phase lag and the amplitude of each disturbance.

Figure 4 shows the mean velocity profile measured by two opposing normal hot-wire probes in laminar flow in the absence of disturbances at $Re = 2280$ and at a distance of 1.82 diameters (i.e. $x/D = 1.82$) from the disturbance generator. The symmetry of the data about the axis can be assessed from this plot because the different symbols represent two families of data obtained at $\phi = 0$ and $\pi$ superposed.

## 3. Results

The pipe and its settling chamber may serve as an acoustic resonator. The resonance frequencies could be estimated assuming an 'organ pipe' having two open ends. The resonance frequencies were found experimentally by measuring the natural disturbances in the pipe. The most significant frequency corresponding to 12 Hz represents half a wavelength of a classic 'organ pipe', which is open at both ends. Linear stability analysis suggests (Garg & Rouleau 1972) that low-frequency disturbances are less stable than high ones and, therefore, those frequencies were chosen for the present investigation. The chosen frequency should not coincide with an acoustically amplified mode and its harmonics. Consequently, a predetermined frequency of 18.5 Hz (dimensionless frequency $\omega = 0.96$) and a Reynolds number of 2280 were selected. The stability characteristics for these flow conditions were calculated by Tumin (1996).

Preliminary experiments established that the axisymmetric mode (azimuthal index $m = 0$) and pure azimuthal periodic modes ($m = 1$ and $m = 2$) did not cause transition at relatively large amplitudes while a combination of modes (e.g. $m = +1$ and $m = -1$ or $m = +2$ and $m = -2$) triggered it at moderately low levels. The observation is consistent with scenario of SSP mentioned in § 1.

The combination of modes $m = +1$ and $m = -1$ or $m = +2$ and $m = -2$ may produce streamwise rolls due to nonlinear interactions, and transition may be triggered at lower amplitudes because the flow becomes unstable with respect secondary disturbances, while the axisymmetric mode and pure azimuthal periodic modes do not generate the streamwise rolls.

It was also established that the system of blowing and suction through neighbouring slots may induce some parasitic helical modes because of interactions between the neighbouring jets. To avoid this interaction and to excite simultaneously clockwise and counter-clockwise helical modes we could activate fewer slots. To excite a combination of helical modes with azimuthal indices $m = +1$ and $m = -1$ one could use only two opposing slots perturbed in anti-phase. This configuration may generate other helical modes with indices $m = \pm 3, \pm 5, \ldots$, (as follows from Fourier analysis) and thus contaminate the signal. Simultaneous excitation of modes $m = +2$ and $m = -2$ through four slots was preferable. In this configuration blowing and suction occur interchangeably through four slots, which are separated by 45°. The disturbances through opposite slots are in phase, while the phase shift between the two pairs is equal to $\pi$. The configuration also generates the helical modes with indices $m = \pm 6, \pm 10, \ldots$, but the contamination of the input signal is much smaller than in the configuration using two slots only. Thus, simultaneous excitation of modes $m = 2$ and $m = -2$ was selected for further analysis.

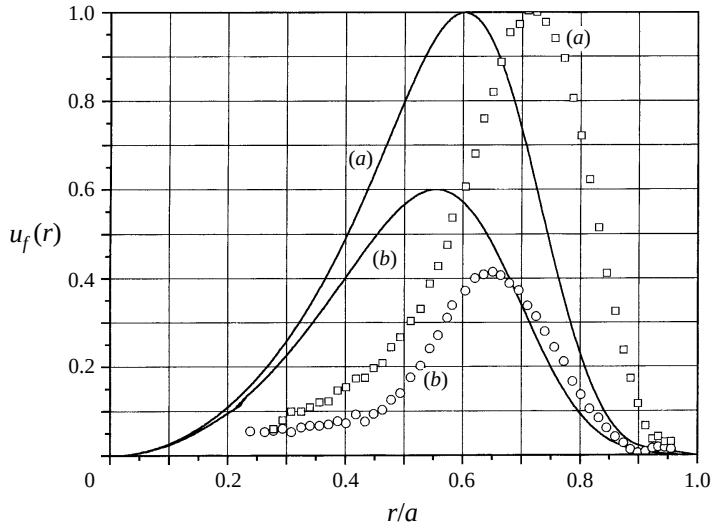


FIGURE 5. The amplitude distribution of the longitudinal velocity component having azimuthal index 2. $f = 18.5$ Hz; $Re = 2280$ ; $C_\mu = 2.57 \times 10^{-5}$. (*a*) $x/D = 1.82$; (*b*) $x/D = 3.3$. Symbols, experiment; lines, theory (Tumin 1996).

The experiments were carried out at three amplitudes. At the smallest amplitude the disturbances decayed in the direction of streaming. At the intermediate amplitude a transient growth of the disturbances was observed to be followed by a decay further downstream. At still higher amplitudes transition to turbulent flow occurred.

### 3.1. *The small-amplitude regime*

The classification of the disturbance amplitudes into the three categories is qualitative only. As a quantitative characteristic of the disturbance amplitude we used the momentum coefficient

$$C_\mu = \frac{2}{U_m^2 a^2} \int_0^a r u_f^2 \, \mathrm{d}r, \tag{3.1}$$

where $u_f(r)$ is the longitudinal velocity disturbance measured at distance $x/D = 1.82$, at $f = 18.5$ Hz and azimuthal indices corresponding to the excited helical modes.

The measurements were done at discrete streamwise distances from the source. The closest section to the source that allows measurements to be made with the hot-wire rake is equal to $x/D = 1.82$. Amplitude distributions of the azimuthal mode $m = 2$ at $x/D = 1.82$ and 3.3 are presented in figure 5. We can see that the maximum of the disturbance shifts toward the centre when the disturbance propagates downstream. A similar result was obtained by Leite (1959). Linear receptivity analysis for the pipe flow with blowing and suction through the surface was carried out by Tumin (1996). The linearized Navier–Stokes equations were solved subject to non-homogeneous boundary conditions on the slot area and the solution was presented as a sum of eigenfunctions corresponding to the prescribed frequency. The result predicts that forcing in the vicinity of the wall generates many eigenmodes and the total amplitude distribution does not correspond to any single eigenmode. Because the more stable eigenmodes have their maxima closer to the wall, the maximum of the total disturbance moves toward the centre where the more slowly decaying

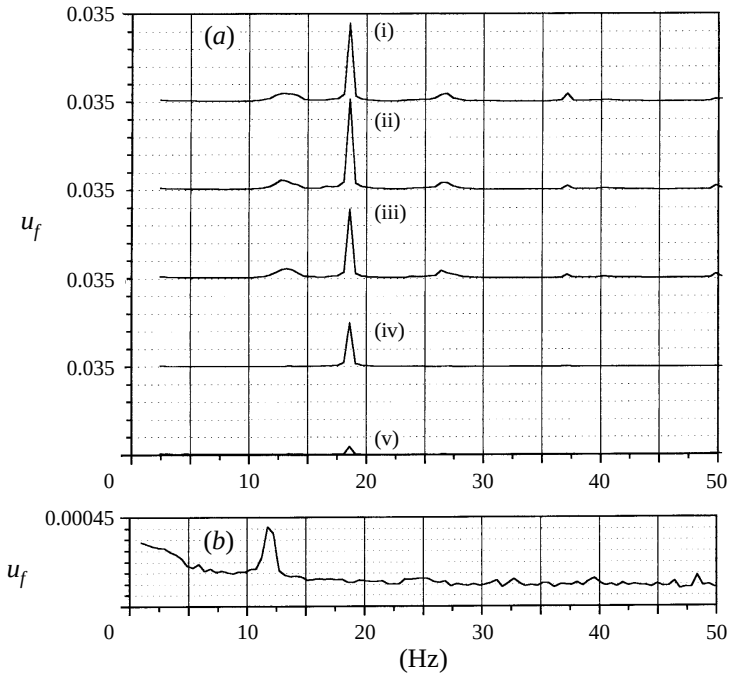


FIGURE 6. Spectra of longitudinal velocity disturbance corresponding to the small-amplitude forcing measured at $r/a = 0.7$; $C_\mu = 7.8 \times 10^{-6}$. (*a*) Excitation of small-amplitude disturbances, (i) $x/D = 0$; (ii) $x/D = 0.61$; (iii) $x/D = 1.21$; (iv) $x/D = 1.82$; (v) $x/D = 3.3$. (*b*) Without excitation.

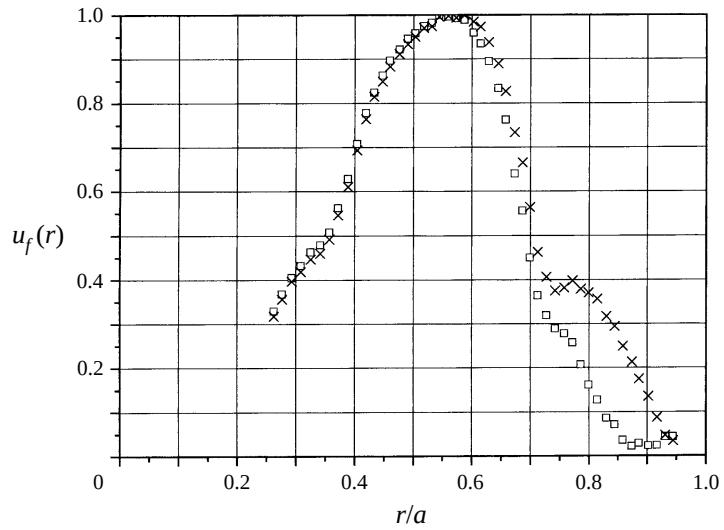


FIGURE 7. The amplitude distribution of the longitudinal velocity component with indices $m = +2$, $C_\mu = 1.84 \times 10^{-4}$ (□) and $m = -2$, $C_\mu = 1.80 \times 10^{-4}$ (×). $f = 18.5$ Hz; $x/D = 1.82$. Intermediate-amplitude forcing.

modes have their maxima. The results of the linear analysis are also presented in figure 5. The matching of the theoretical and experimental results was done by the maximum value of $u_f$ measured at $x/D = 1.82$. Although the theoretical results agree qualitatively with the experiment, the radial location of the theoretical

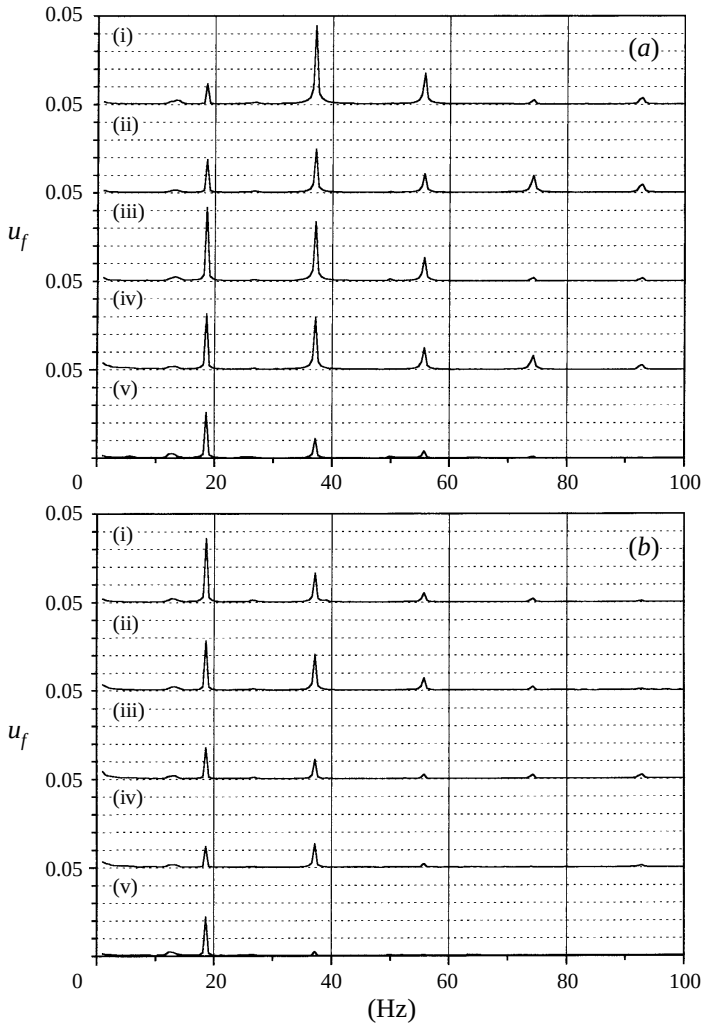


FIGURE 8. Intermediate-amplitude forcing. Spectra of the disturbance measured at $r/a = 0.5$, $C_\mu = 1.84 \times 10^{-4}$. (*a*) In the meridional section of the active slots; (*b*) opposite idle slots. $x/D =$ 1.82 (i); 3.3 (ii); 4.3 (iii); 5.23 (iv); 14 (v).

maximum is closer to the centre. Because of experimental difficulties we could not measure the velocity distribution in the immediate vicinity of the slot during the entire disturbance cycle. Thus, in the theoretical model a step velocity profile was assumed exist in the slots. We attribute the disparity between the experimental and theoretical results to a difference between the theoretical and experimental velocity profiles.

Modal decomposition of the data indicated that the velocity amplitudes of modes $m = 1$ and 3 are about 5 times smaller than the amplitude of the mode $m = 2$. The spectral distribution of the total signal near the location of the peak amplitude (i.e. at $r/a = 0.7$) is presented in figure 6(*a*). To measure the disturbance closer to the slot (at $x/D < 1.82$) we replaced the rake with a single wire. A spectrum measured in the absence of forcing is also shown in figure 6(*b*). The observed peak in the spectrum corresponds to the acoustic resonance frequency of approximately 12 Hz inherent in

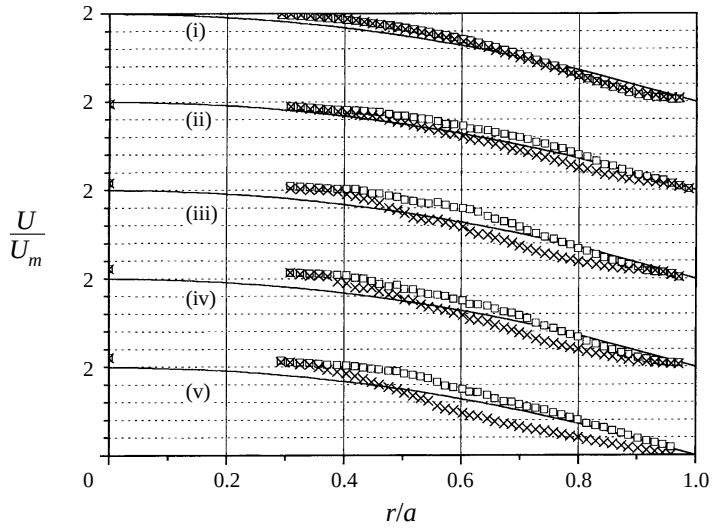


FIGURE 9. Intermediate amplitude of forcing. Mean velocity profiles in the two meridional sections and at different distances from the slots. $C_\mu = 1.84 \times 10^{-4}$: $\times$, in the section opposite active slots; $\square$, opposite idle slots. $x/D = 1.82$ (i); 3.3 (ii); 4.3 (iii); 5.23 (iv); 14 (v). Line, the parabolic profile.

the system. Secondary peaks at a frequencies of 13 and 26 Hz (figure 6*a*, locations (i)–(iii)) are caused by the vibration of the long probe holder. When the experiment was repeated with a shorter holder these peaks disappeared, while the peak at 12 Hz remained (the latter cannot be seen in figure because of the large amplitude scale).

From figure 6(*a*) we can also see that there is, at least, an order of magnitude difference between the fundamental frequency and its immediate harmonics.

### 3.2. *The intermediate-amplitude regime*

The amplitude distributions of the azimuthal modes measured at 18.5 Hz with indices $m = \pm 2$ measured at 1.82 diameters downstream of the slots are shown in figure 7. These modes have broad maxima stretching between $r/a = 0.45$ and 0.65. Other azimuthal modes with indices $m = 0, \pm 1, \pm 3$ also have broad maxima at the same interval of $r/a$. The resultant amplitude of all other azimuthal modes at this distance is as large as 50–60 % of the forced modes with azimuthal indices $\pm 2$. All of these modes experience a clear transient growth.

Because the maximum of the velocity disturbance occurs at $r/a$ about 0.5, the coordinate $r/a = 0.49$ was chosen for the measurements of spectra. The spectra of the streamwise velocity component at different streamwise locations are shown in figure 8. There are two sets of data. The first one was obtained at a meridional section corresponding to an active slot while the second one was obtained opposite an inactive slot (i.e. between two pairs of the slots with blowing and suction). We can see a clear transient growth at the forced frequency of 18.5 Hz in the set measured opposite the active slots. An increase in the amplitude of the fundamental frequency may be observed at $x/D > 3.3$ which is followed by a decay at $x/D > 4.3$. A transient growth opposite the inactive slot (figure 8*b*) occurred farther downstream (i.e. at $x/D > 5.23$). The higher harmonics in this regime are comparable in amplitude to the fundamental. The mean velocity profile becomes distorted in a non-axisymmetric

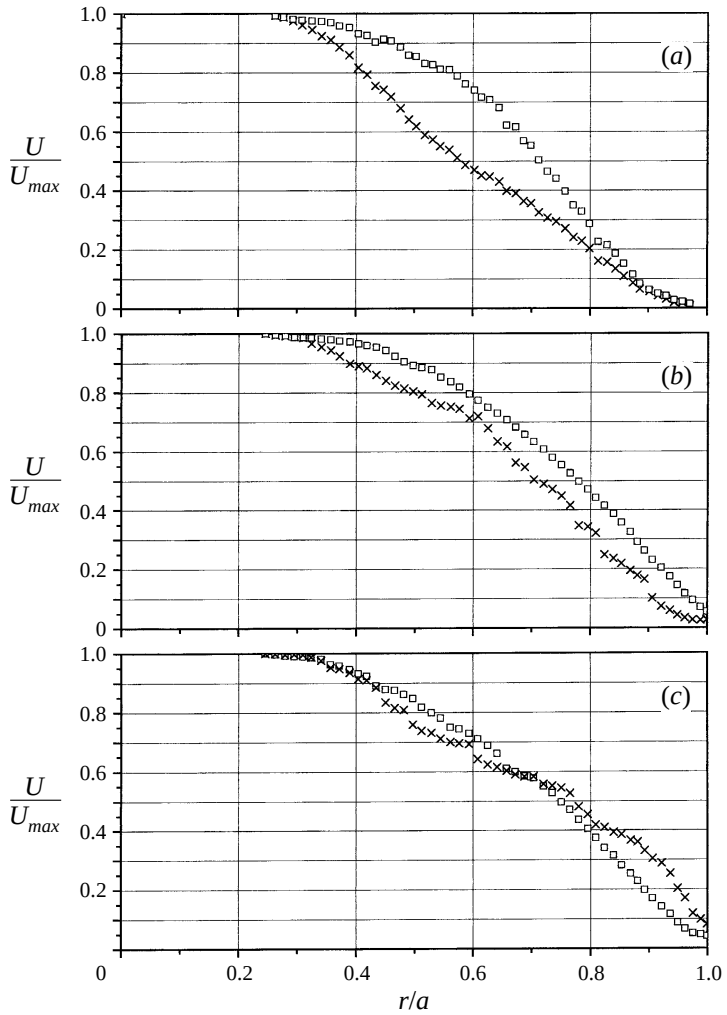


FIGURE 10. Intermediate-amplitude forcing. Mean velocity profiles in the two meridional sections at $x/D = 7.3$: $\times$, in the meridional section of the active slots; $\square$, opposite idle slots. (*a*) The basic configuration; (*b*) additional phase shift between two pairs of slots is equal to $\pi/8$; (*c*) additional phase shift is equal to $\pi/4$.

manner. Figure 9 shows the evolution of the mean velocity profiles in the two meridional sections. The differences between these mean velocity profiles indicate that longitudinal vortical structures must exist in the flow. These vortices redistribute the longitudinal momentum and produce an azimuthal variation of the longitudinal velocity component $U(x, r, \theta)$. In boundary layer and channel flows the spanwise variations of the longitudinal velocity component are commonly referred to as streaks. The streaky flow $U(x, r, \theta)$ contains azimuthal inflection points, and it may be unstable with respect to secondary three-dimensional disturbances as is suggested by the SSP scenario.

Although we present data obtained by two probes only, other measurements indicated that the results are symmetrical for each pair of meridional sectors. Thus, other pairs of probes located at similar sections gave identical results.

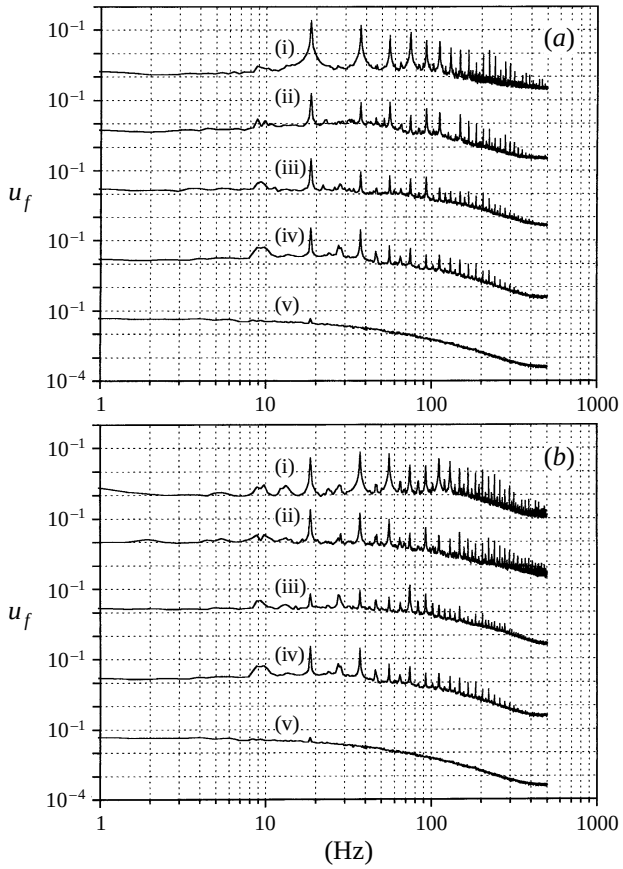


FIGURE 11. High amplitude of forcing. Spectra of the disturbance measured at $r/a = 0.5$; $C_\mu = 3.4 \times 10^{-3}$: (*a*) in the meridional section of the active slots; (*b*) opposite idle slots. $x/D =$ 1.82 (i); 3.3 (ii); 4.3 (iii); 5.23 (iv); 14 (v).

A crucial question is associated with the genesis of the mean velocity distortion. It may occur due to nonlinear interaction between the induced strong disturbances. Long & Petersen (1992) showed that nonlinear interactions between two helical waves having azimuthal indices $m = +2$ and $m = -2$ distort the mean flow in an axisymmetric jet with azimuthal index of $m = 4$. Perhaps a similar nonlinear process exists in the pipe when the amplitudes are sufficiently large.

Changing the phase shifts between azimuthal modes from 0 to $\pi/8$ and later $\pi/4$ have resulted in different mean velocity profiles (figure 10). It suggests that the mean velocity distortion is a consequence of the nonlinear interactions among the high-amplitude disturbances induced in the flow.

### 3.3. *The high-amplitude regime*

The disturbance spectra of the longitudinal velocity component forced at high amplitude are shown in figure 11, and the corresponding mean velocity profiles are shown in figure 12. The spectrum at $x/D = 1.82$ contains strong higher harmonics and mean velocity distortion is significant as well. A subharmonic disturbance which is most pronounced at the meridional sections located between the active slots occurs in this flow regime. Far downstream all frequencies are amplified and the spectrum

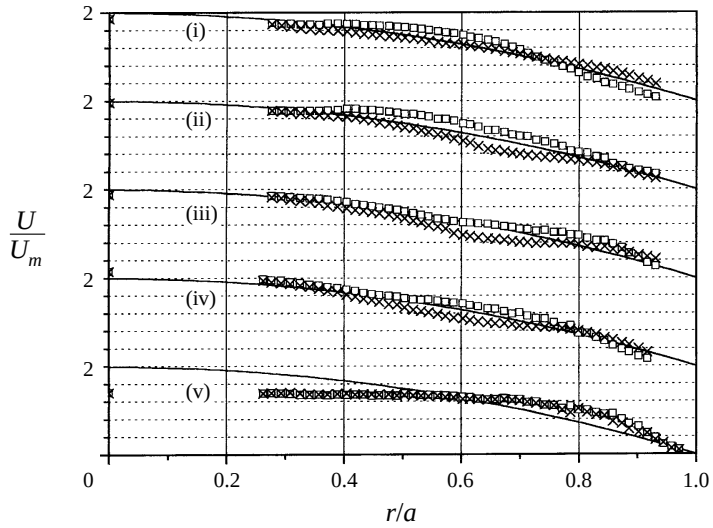


FIGURE 12. High amplitude of forcing. Mean velocity profiles in the two meridional sections and at different distances from the slots. $C_\mu = 3.4 \times 10^{-3}$: $\times$, in the section of active slots; $\square$, opposite idle slots. $x/D = 1.82$ (i); 3.3 (ii); 4.3 (iii); 5.23 (iv); 14 (v). Line, the parabolic profile.

represents turbulent flow. We have compared the ensuing turbulent spectrum with the spectrum resulting from transition caused at the inlet. The spectra are very similar. In order to prove the turbulent character of the flow, we have analysed the mean velocity profiles as well. The profiles satisfy the law of the wall and the velocity defect law, which are well documented in turbulent pipe flow at higher Reynolds numbers.

### 3.4. *The pipe flow with stationary jets*

Since mean velocity distortion preceded transition to turbulence in our experiment, and it suggests the presence of streamwise rolls, we speculate that it is an important stage in the general process, as is the case in the SSP scenario (see § 1). We thus introduced a steady weak secondary flow into the pipe through four alternate slots in order to emulate a mean velocity distortion by streamwise rolls with an azimuthal index of 4. The resulting mean velocity profiles measured at two meridional sections at $x/D = 7.3$ are plotted in figure 13(*a*). The mean velocity disturbance is small and the velocity profiles are close to parabolic. Periodic disturbances of small amplitude were added in order to assess the role of the small mean velocity distortion in the amplification process. The periodic disturbances in the absence of jets also have a small influence on the mean velocity profiles (see figure 13*b*). The simultaneous effect of the constant jets and the small periodic disturbances is shown in figure 13(*c*). Spectral analysis has also shown that the periodic disturbance in the presence of the initial mean velocity distortion is amplified. It suggests that the streamwise rolls support the amplification of the disturbance while the disturbance amplifies these stationary rolls. A comparison between the velocity profiles obtained without jets but at a large amplitude of the disturbance and with the jets in combination with much smaller disturbance amplitude is shown in figure 14. It can be seen that the mean velocity profiles are very similar in both cases. Thus, the constant jets really help to emulate the mean velocity distortion mechanism observed in the

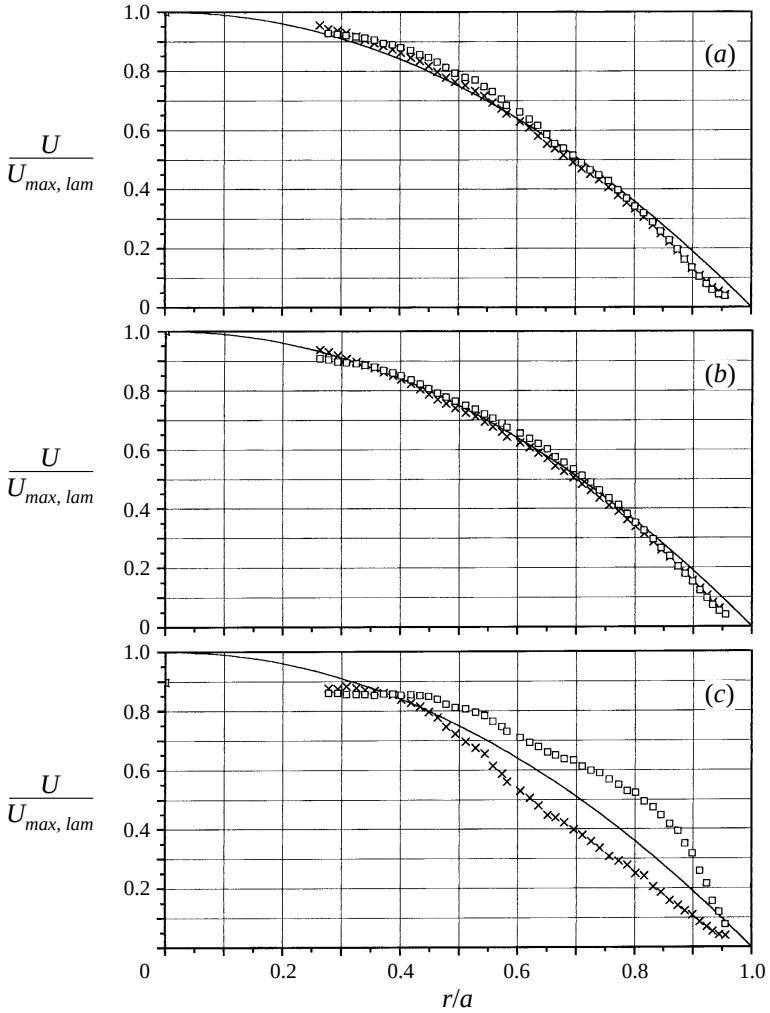


FIGURE 13. Mean velocity profiles at $x/D = 7.3$. (*a*) In the presence of four jets; (*b*) in the presence of only periodic disturbances ($m = +2$ and $m = -2$); (*c*) four jets and the periodic disturbances are induced through the four slots. Line, parabola; symbols, experimental data. ×, In the meridional section of the active slots; □, opposite idle slots.

previous experiments. Far downstream, transition to turbulence was observed in both cases.

## 4. Summary

These experimental results suggest that transition to turbulence in a fully developed Poiseuille pipe flow can occur only after the parabolic velocity profile became distorted. The longitudinal vortices associated with such a distortion can be generated either by a steady or by a periodic disturbance (due to nonlinear interactions). The mean flow distorted by the introduction of finite streamwise rolls becomes unstable to secondary azimuthal periodic disturbances. The modulation is also amplified by the presence of the periodic disturbances. Our results are consistent with the SSP scenario and numerical simulations by Nikitin (1994, 1995) and Zikanov (1996). In this connection

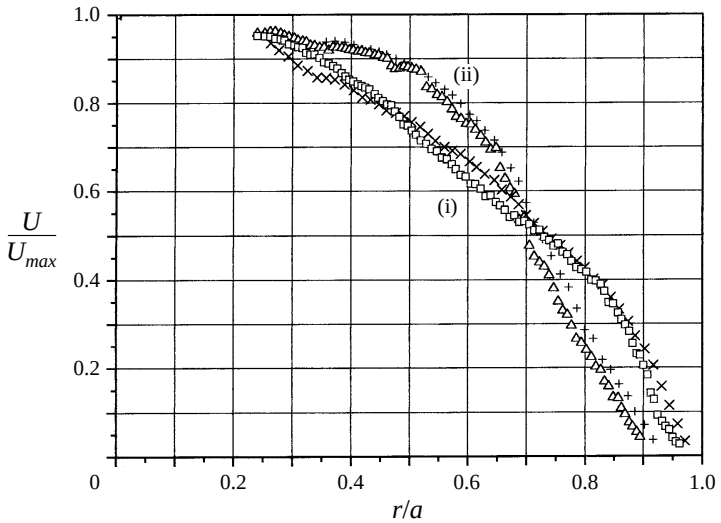


FIGURE 14. Mean velocity profiles in the pipe flow obtained in the experiments with big disturbance amplitudes and mean velocity profiles when disturbance of intermediate amplitude is excited in presence of the jets. $x/D = 1.82$. (i) In the meridional section of the active slots; (ii), opposite idle slots. +, △, In the meridional section of the active slots (big amplitude of the disturbance without jets and intermediate amplitude disturbance with jets respectively); □, ×, opposite idle slots (without jets and with jets respectively).

we expect that a weakly nonlinear analysis of the pipe flow distorted by streamwise rolls will explain a regeneration of the rolls and, therefore, a mechanism of transition in Poiseuille pipe flow.

The authors would like to thank Professor M. Sokolov and Dr A. Seifert for useful discussions and for their helpful suggestions during this work. A. Tumin acknowledges the financial support in the form of Guastela scholarship from the Rashi foundation. The work was supported by the Israel Science Foundation.

## REFERENCES

BERGSTRÖM, L. 1992 Initial algebraic growth of small angular dependent disturbances in pipe Poiseuille flow. *Stud. Appl. Maths* **87**, 61–79.

BERGSTRÖM, L. 1993*a* Optimal growth of small disturbances in pipe Poiseuille flow. *Phys. Fluids* A **5**, 2710–2719.

BERGSTRÖM, L. 1993*b* Evolution of laminar disturbances in pipe Poiseuille flow. *Eur. J. Mech.* B/*Fluids* **12**, 749–768.

BOBERG, L. & BROSA, U. 1988 Onset of turbulence in a pipe. *Z. Naturforsch.* **43a**, 697–726.

CHRISTIANSEN, E. B. & LEMMON, H. E. 1965 Entrance region flow. *AICHE J.* **11**, 995–999.

COHEN, J. & WYGNANSKI, I. 1987 The evolution of instabilities in the axisymmetric jet. Part 1. The linear growth of disturbances near the nozzle. *J. Fluid Mech.* **176**, 191–219.

DARBYSHIRE, A. G. & MULLIN, T. 1995 Transition to turbulence in constant-mass-flux pipe flow. *J. Fluid Mech.* **289**, 83–114.

DRAZIN, P. G. & REID, W. H. 1981 *Hydrodynamic Stability*. Cambridge University Press.

FOX, J. A., LESSEN, M. & BHAT, W. V. 1968 Experimental investigation of the stability of Hagen-Poiseuille flow. *Phys. Fluids* **11**, 1–4.

GARG, V. K. & ROULEAU, W. T. 1972 Linear stability of pipe Poiseuille flow. *J. Fluid Mech.* **54**, 113–127.

GOLDSTEIN, S. 1938 *Modern Developments in Fluid Dynamics*, vol. 1. pp. 301–308. Oxford University Press.

GUSTAVSSON, L. H. 1989 Direct resonance of nonaxisymmetric disturbances in pipe flow. *Stud. Appl. Maths* **80**, 95–108.

KASKEL, A. 1961 Experimental study of the stability of pipe flow. II. Development of disturbance generator. *Jet Propulsion Laboratory Tech. Rep.* 32–138. Pasadena, California.

LEITE, R. J. 1959 An experimental investigation of the stability of Poiseuille flow. *J. Fluid Mech.* **5**, 81–97.

LONG, T. A. & PETERSEN, R. A. 1992 Controlled interactions in a forced axisymmetric jet. Part 1. The distortion of the mean flow *J. Fluid Mech.* **235**, 37–55.

MAYER, E. W. & RESHOTKO, E. 1997 Evidence for transient disturbance growth in a 1961 pipe-flow experiment. *Phys. Fluids* **9**, 242–244.

MORKOVIN, M. V. & RESHOTKO, E. 1990 Dialogue on progress and issues in stability and transition research. In *Laminar-Turbulent Transition, IUTAM Symp. Toulouse* (ed. D. Arnal & R. Michel), pp. 1–29. Springer.

NIKITIN, N. V. 1994 Direct numerical modeling of three-dimensional turbulent flows in pipes of circular cross section. *Fluid Dyn.* **29**, 749–758.

NIKITIN, N. V. 1995 Spatial approach to numerical modeling of turbulence in pipe flows. *Physics–Dok.* **40**, 434–437.

PFENINGER, W. 1961 Transition in the inlet length of tubes at high Reynolds numbers In *Boundary Layer and Flow Control* (ed. G. V. Lachman), pp. 970–980. Pergamon.

RESHOTKO, E. 1958 Experimental study of the stability of pipe flow. I. Establishment of an axially symmetric Poiseuille flow. *Jet Propulsion Laboratory, Progress Rep.* 20-364. Pasadena, California.

REYNOLDS, O. 1883 An experimental investigation of the circumstances which determine whether the motion of water shall be direct or sinuous, and of the law of resistance in parallel channels. *Phil. Trans. R. Soc. Lond.* **174**, 935–982.

RUBIN, Y., WYGNANSKI, I. J. & HARTIONIDIS, J. H. 1980 Further observation on transition in a pipe. In *Laminar-Turbulent Transition, IUTAM Symp. Stuttgart* (ed. R. Eppler & H. Fasel), pp. 19–26. Springer.

SCHMID, P. J. & HENNINGSON, D. S. 1994 Optimal energy density growth in Hagen-Poiseuille flow. *J. Fluid Mech.* **277**, 197–225.

TATSUMI, T. 1952 Stability of the laminar inlet-flow prior to the formation of Poiseuille regime, Part II. *J. Phys. Soc. Japan* **7**, 495–502.

TUMIN, A. 1996 Receptivity of pipe Poiseuille flow. *J. Fluid Mech.* **315**, 119–137.

WALEFFE, F. 1995*a* Hydrodynamic stability and turbulence: Beyond transients to a self-sustaining process. *Stud. Appl. Maths* **95**, 319–343.

WALEFFE, F. 1995*b* Transition in shear flows. Nonlinear normality versus non-normal linearity. *Phys. Fluids* **7**, 3060–3066.

WALEFFE, F. 1996 On self-sustaining process in shear flows. *Phys. Fluids* **9**, 883–900.

WYGNANSKI, I. & CHAMPAGNE, F. H. 1973 On transition in a pipe flow. *J. Fluid Mech.* **59**, 281–335.

WYGNANSKI, I., SOKOLOV, M. & FRIEDMAN, D. 1975 On transition in a pipe. Part 2. The equilibrium puff. *J. Fluid Mech.* **69**, 283–304.

ZIKANOV, O. YU. 1996 On the stability of pipe Poiseuille flow. *Phys. Fluids* **9**, 2923–2932.